JOURNAL OF Applied Polymer SCIENCE

Special Issue: Bio-based Packaging

Guest Editors: José M. Lagarón, Amparo López-Rubio, and María José Fabra
Institute of Agrochemistry and Food Technology of the Spanish Council for Scientific Research

EDITORIAL

REVIEWS

RESEARCH ARTICLES

JOURNAL OF Applied Polymer SCIENCE

Special Issue: Bio-based Packaging

Guest Editors: José M. Lagarón, Amparo López-Rubio, and María José Fabra
Institute of Agrochemistry and Food Technology of the Spanish Council for Scientific Research

Impact of fermentation residues on the thermal, structural, and rheological properties of polyhydroxy(butyrate-*co*-valerate) produced from cheese whey and olive oil mill wastewater
L. Hilliou, D. Machado, C. S. S. Oliveira, A. R. Gouveia, M. A. M. Reis, S. Campanari, M. Villano and M. Majone, *J. Appl. Polym. Sci.* 2015, DOI: 10.1002/app.42818

Synergistic effect of lactic acid oligomers and laminar graphene sheets on the barrier properties of polylactide nanocomposites obtained by the in situ polymerization pre-incorporation method
J. Ambrosio-Martín, A. López-Rubio, M. J. Fabra, M. A. López-Manchado, A. Sorrentino, G. Gorrasi and J. M. Lagarón, *J. Appl. Polym. Sci.* 2015, DOI: 10.1002/app.42661

Antibacterial poly(lactic acid) (PLA) films grafted with electrospun PLA/allyl isothiocyanate fibers for food packaging
H. H. Kara, F. Xiao, M. Sarker, T. Z. Jin, A. M. M. Sousa, C.-K. Liu, P. M. Tomasula and L. Liu, *J. Appl. Polym. Sci.* 2015, DOI: 10.1002/app.42475

Poly(L-lactide)/ZnO nanocomposites as efficient UV-shielding coatings for packaging applications
E. Lizundia, L. Ruiz-Rubio, J. L. Vilas and L. M. León, *J. Appl. Polym. Sci.* 2015, DOI: 10.1002/app.42426

Effect of electron beam irradiation on the properties of polylactic acid/montmorillonite nanocomposites for food packaging applications
M. Salvatore, A. Marra, D. Duraccio, S. Shayanfar, S. D. Pillai, S. Cimmino and C. Silvestre, *J. Appl. Polym. Sci.* 2015, DOI: 10.1002/app.42219

Preparation and characterization of linear and star-shaped poly L-lactide blends
M. B. Khajeheian and A. Rosling, *J. Appl. Polym. Sci.* 2015, DOI: 10.1002/app.42231

Mechanical properties of biodegradable polylactide/poly(ether-block-amide)/thermoplastic starch blends: Effect of the crosslinking of starch
L. Zhou, G. Zhao and W. Jiang, *J. Appl. Polym. Sci.* 2015, DOI: 10.1002/app.42297

Interaction and quantification of thymol in active PLA-based materials containing natural fibers
I. S. M. A. Tawakkal, M. J. Cran and S. W. Bigger, *J. Appl. Polym. Sci.* 2015, DOI: 10.1002/app.42160

Graphene-modified poly(lactic acid) for packaging: Material formulation, processing, and performance
M. Barletta, M. Puopolo, V. Tagliaferri and S. Vesco, *J. Appl. Polym. Sci.* 2015, DOI: 10.1002/app.42252

Edible films based on chia flour: Development and characterization
M. Dick, C. H. Pagno, T. M. H. Costa, A. Gomaa, M. Subirade, A. De O. Rios and S. H. Flóres, *J. Appl. Polym. Sci.* 2015, DOI: 10.1002/app.42455

Influence of citric acid on the properties and stability of starch-polycaprolactone based films
R. Ortega-Toro, S. Collazo-Bigliardi, P. Talens and A. Chiralt, *J. Appl. Polym. Sci.* 2015, DOI: 10.1002/app.42220

Bionanocomposites based on polysaccharides and fibrous clays for packaging applications
A. C. S. Alcântara, M. Darder, P. Aranda, A. Ayral and E. Ruiz-Hitzky, *J. Appl. Polym. Sci.* 2015, DOI: 10.1002/app.42362

Hybrid carrageenan-based formulations for edible film preparation: Benchmarking with kappa carrageenan
F. D. S. Larotonda, M. D. Torres, M. P. Gonçalves, A. M. Sereno and L. Hilliou, *J. Appl. Polym. Sci.* 2015, DOI: 10.1002/app.42263

JOURNAL OF Applied Polymer SCIENCE

Special Issue: Bio-based Packaging

Guest Editors: José M. Lagarón, Amparo López-Rubio, and María José Fabra
Institute of Agrochemistry and Food Technology of the Spanish Council for Scientific Research

Structural and mechanical properties of clay nanocomposite foams based on cellulose for the food packaging industry
S. Ahmadzadeh, J. Keramat, A. Nasirpour, N. Hamdami, T. Behzad, L. Aranda, M. Vilasi and S. Desobry, *J. Appl. Polym. Sci.* 2015, DOI: 10.1002/app.42079

Mechanically strong nanocomposite films based on highly filled carboxymethyl cellulose with graphene oxide
M. El Achaby, N. El Miri, A. Snik, M. Zahouily, K. Abdelouahdi, A. Fihri, A. Barakat and A. Solhy, *J. Appl. Polym. Sci.* 2015, DOI: 10.1002/app.42356

Production and characterization of microfibrillated cellulose-reinforced thermoplastic starch composites
L. Lendvai, J. Karger-Kocsis, Á. Kmetty and S. X. Drakopoulos, *J. Appl. Polym. Sci.* 2015, DOI: 10.1002/app.42397

Development of bioplastics based on agricultural side-stream products: Film extrusion of *Crambe abyssinica*/wheat gluten blends for packaging purposes
H. Rasel, T. Johansson, M. Gällstedt, W. Newson, E. Johansson and M. Hedenqvist, *J. Appl. Polym. Sci.* 2015, DOI: 10.1002/app.42442

Influence of plasticizers on the mechanical and barrier properties of cast biopolymer films
V. Jost and C. Stramm, *J. Appl. Polym. Sci.* 2015, DOI: 10.1002/app.42513

The effect of oxidized ferulic acid on physicochemical properties of bitter vetch (*Vicia ervilia*) protein-based films
A. Arabestani, M. Kadivar, M. Shahedi, S. A. H. Goli and R. Porta, *J. Appl. Polym. Sci.* 2015, DOI: 10.1002/app.42894

Effect of hydrochloric acid on the properties of biodegradable packaging materials of carboxymethylcellulose/poly(vinyl alcohol) blends
M. D. H. Rashid, M. D. S. Rahaman, S. E. Kabir and M. A. Khan, *J. Appl. Polym. Sci.* 2015, DOI: 10.1002/app.42870

Journal of Applied Polymer Science

Bionanocomposites based on polysaccharides and fibrous clays for packaging applications

Ana C. S. Alcântara,[1]* Margarita Darder,[1] Pilar Aranda,[1] André Ayral,[2] Eduardo Ruiz-Hitzky[1]
Instituto de Ciencia de Materiales de Madrid, CSIC, Cantoblanco, Madrid E-28049, Spain
Institut Européen des Membranes, CNRS-ENSCM-UM, CC47, Université de Montpellier, Montpellier F-34095, CEDEX 5, France
*Present address: Universidade Federal do Rio Grande do Norte, UFRN, Departamento de Química-LABPEMOL, Lagoa Nova 59072-970 Natal-RN, Brasil
Correspondence to: E. Ruiz-Hitzky (E-mail: eduardo@icmm.csic.es)

ABSTRACT: The present paper reports the use of sepiolite and palygorskite fibrous clays as fillers to improve the mechanical and barrier properties of films based on neutral or negatively charged polysaccharides, such as hydroxypropylmethylcellulose, carboxymethylcellulose, alginate, pectin, and xanthan. The interaction established between the polysaccharide chains and the clay fibers, as well as the physicochemical characteristics of the resulting bionanocomposites are characterized by several techniques. These materials are processed as self-standing films that not only exhibit improved mechanical properties and water resistance, but also a significant barrier to UV light and reduced water absorption capacity, which make them very attractive for use in food packaging or coatings. Moreover, fibrous clays previously modified with the hydrophobic protein zein are also evaluated as fillers in alginate matrices, focusing on the improvement of water resistance, as well as of light and gas barrier properties, especially towards oxygen, which are of special interest for potential application in the food packaging sector. © 2015 Wiley Periodicals, Inc. J. Appl. Polym. Sci. **2016**, *133*, 42362.

KEYWORDS: biopolymers and renewable polymers; clay; composites; packaging; polysaccharides

Received 5 February 2015; accepted 13 April 2015
DOI: 10.1002/app.42362

INTRODUCTION

Natural polymers, such as polysaccharides and proteins, are receiving considerable attention for the development of green plastics, as an ecological alternative to common petroleum-based plastics. This is due to their availability, low cost, high biocompatibility and biodegradability, as well as good film-forming ability and flexibility in most cases.[1,2] Polysaccharides, which are composed of long chains of monosaccharide units joined together by glycosidic linkages, are an interesting source for the development of green and renewable materials due to their profusion in the biosphere.[3,4] However, films based on these macromolecules show relatively poor mechanical properties, low stability in aqueous media and very low water barrier properties due to their high hydrophilicity. For this reason, much work is still needed to overcome these drawbacks in order to enlarge the applications range, even in wet environmental conditions.

With the aim to accomplish the requirements of the packaging sector, the use of clay minerals as fillers of polysaccharides and other biodegradable polymers is a common strategy followed to improve the mechanical and barrier properties of these matrices, as well as their solvent resistance.[3,5–11] Although most of the work developed in this research topic has been focused on the use of layered silicates, other natural silicates with fibrous morphology like sepiolite and palygorskite have emerged in the last years as promising fillers in the development of bionanocomposite materials.[4,12–17] The crystalline structure of these naturally occurring clays consists of discontinuous phyllosilicate layers arranged parallel to the fiber direction (c-axis), resulting in structural blocks alternating with structural cavities (tunnels) [Figure 1(a)]. Each block contains two tetrahedral silica sheets sandwiching a central sheet of magnesium hydroxide, which can contain isomorphous substitutions of Al^{3+} or other trivalent cations, especially in the case of palygorskite.[18,19] The ideal unit cell formula is $(Si_{12}O_{30}Mg_8(OH)_4(H_2O)_4{\cdot}8H_2O)$ in sepiolite, and $(Si_8O_{20}Mg_5(OH)_2(H_2O)_4{\cdot}4H_2O)$ in the case of palygorskite. The fiber length is typically less than 5 μm in sepiolite, although it depends on its origin and the fibers can be much longer in certain cases. Palygorskite fibers are also often below 5 μm length, but this value can reach up to 20 μm in palygorskites of hydrothermal origin. Together with the large porosity and high specific surface area of these fibrous clays, an interesting feature is the presence of silanol groups located on the external surface,

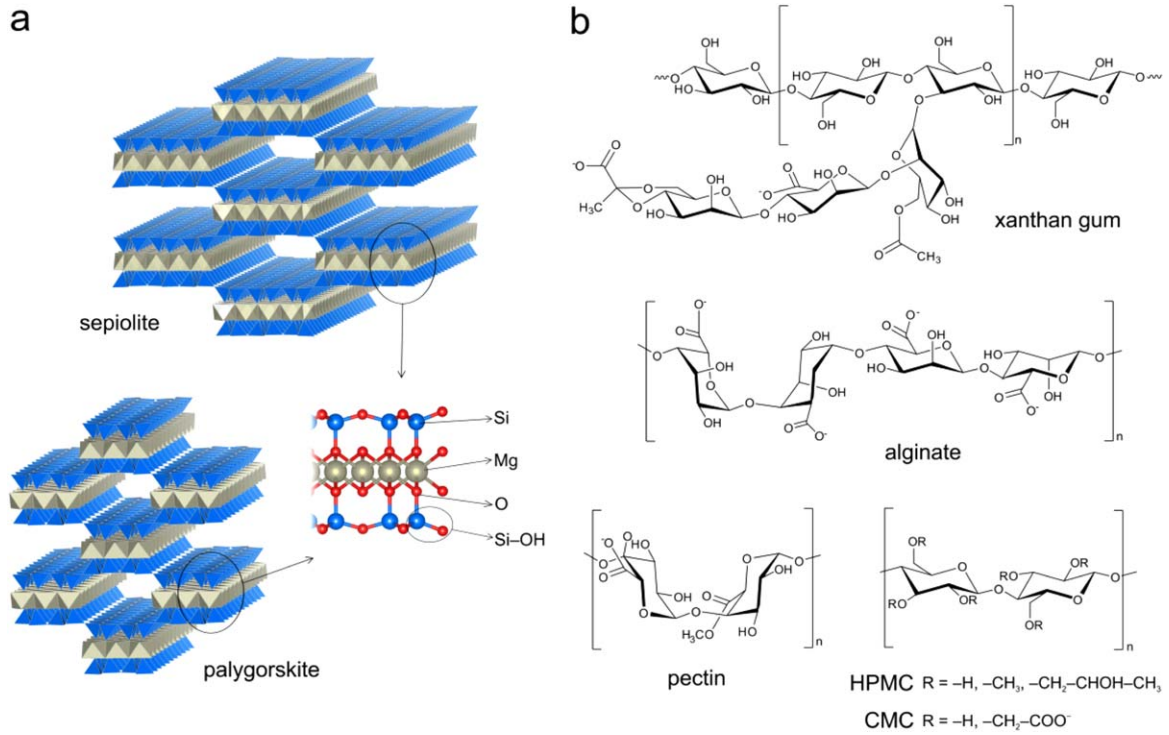

Figure 1. Chemical structure of the (a) fibrous clay minerals and (b) polysaccharides used in this work. [Color figure can be viewed in the online issue, which is available at wileyonlinelibrary.com.]

which can act as sites for interactions with biopolymers leading to the improved stability in water as well as better mechanical and barrier properties in the resulting bionanocomposites.[4,12,14,16,17,20] The abundancy of these hydroxyl groups in fibrous clays favors the interaction through hydrogen bonding with all type of polysaccharides or other biomacromolecules, even those neutral or bearing negative charges.[15,17,20,21] In fact, certain anionic polysaccharides like alginate, pectin and carrageenan have shown good interaction with layered double hydroxides, the so-called anionic clays or hydrotalcite-type clays,[22] but their interaction through electrostatic interaction with the negatively charged sites of smectites and fibrous clays minerals is limited due to the lack of positive charges.

Fibrous clay minerals can be also modified with diverse organic compounds in order to provide them with additional properties, giving rise to hybrid materials commonly known as organoclays.[23–25] Alkylammonium organic cations have been usually employed to modify clay minerals and provide them with hydrophobic behavior, but they are not appropriate as fillers in plastics for food packaging due to their inherent toxicity. Thus, biological compounds like phospholipids[26,27] or the corn protein zein[15] have been introduced as interesting ecological alternatives to alkylammonium cations, being safe for application in the food sector. Zein is well known for its strong hydrophobicity and barrier properties towards water vapor and oxygen,[28–32] and it has been assembled to sepiolite and palygorskite with the aim to reduce the hydrophilic character of both clays[15] and enhance the solvent resistance and the moisture barrier of the biopolymer films reinforced with these modified clays.

In the current work, sepiolite and palygorskite fibrous clays were evaluated as reinforcing fillers to improve the mechanical and barrier properties of films based on neutral or negatively charged polysaccharides, such as hydroxypropylmethylcellulose, carboxymethylcellulose, alginate, pectin, and xanthan, whose chemical structures are depicted in Figure 1(b). The properties of the resulting bionanocomposite films were evaluated focusing on their mechanical properties, water resistance, and light barrier properties, due to the interest of these bio-based materials in the packaging sector. For comparison, alginate matrices reinforced with zein-modified fibrous clays were also evaluated, with special emphasis on the improvement of water resistance, as well as light, moisture and gas barrier properties, which are crucial for application of these films in food packaging.

EXPERIMENTAL

Materials

Sepiolite from Vicálvaro (Spain), commercialized as Pangel S9 (SEP), was provided by TOLSA, S.A., and Brazilian palygorskite (PALY) from the Piauí state was kindly provided by Prof. L.S. Barreto (Universidade Federal de Sergipe). The polysaccharides sodium alginate (ALG; alginic acid sodium salt from brown algae), xanthan gum (XG; from *Xanthomonas campestris*), carboxymethylcellulose (CMC; carboxymethylcellulose sodium salt, medium viscosity), hydroxypropylmethylcellulose (HPMC; viscosity 40–60 cP, 2% in H_2O, 20°C), and pectin (PCT; from citrus fruits, galacturonic acid content 87.6%), as well as the corn protein zein (Z) were purchased from Sigma-Aldrich. This protein is presented as a yellow powder and was reported to be approximately 35% α-zein, which includes two sub-units of

average molecular weight of 22 and 24 kDa (Sigma-Aldrich product information). Absolute ethanol was obtained from Panreac and $CaCl_2$ ($\geq$ 99%) from Fluka. Deionized water (resistivity of 18.2 MΩ cm) was obtained with a Maxima Ultrapure Water from Elga.

Preparation of Polysaccharide-Fibrous Clays Bionanocomposite Films

A series of polysaccharide films reinforced with different amounts of sepiolite or palygorskite with respect to biopolymer mass (3, 17, 33, or 50% (w/w)) were prepared. For the ALG, XG, PCT and CMC bionanocomposite films, a 2% (w/v) aqueous biopolymer solution was first prepared at 60°C. Then, an aqueous clay suspension (2% w/v) was slowly added to the biopolymer solution under magnetic stirring in order to form a single batch that is kept under constant stirring until complete homogenization. The HPMC films loaded with sepiolite or palygorskite were prepared using a similar procedure, but using cold water for the dissolution of the polysaccharide. In all cases, the resulting polysaccharide-fibrous clay suspensions were finally placed onto Petri dishes and allowed to dry at room temperature.

Preparation of Alginate Bionanocomposite Films Using Zein-Fibrous Clays as Filler

The biohybrid zein-fibrous clay fillers were prepared following the reported procedure:[15] suspensions of sepiolite or palygorskite (6 g L^{-1}) were prepared in 80% (v/v) ethanol/water, being vigorously stirred by means of a mixer (G2 model, Lomi) to properly disperse the clay. Different amounts of zein were dissolved in 50 mL of 80% (v/v) ethanol/water in order to prepare a set of solutions with zein concentration ranging between 0.6 and 30 g L^{-1}. Each zein solution was then added to the sepiolite or palygorskite dispersion, and this single batch was kept under magnetic stirring for 48 h. Then, the solid product was isolated by centrifugation (40 min, 8000 rpm) and subsequently dried overnight at 40°C. The resulting zein-sepiolite and zein-palygorskite biohybrid materials were denoted as Z-SEP# and Z-PALY#, respectively, where # refers to the amount of zein (g) per 100 g of clay in each biohybrid calculated from chemical analysis.

In a second step, alginate films loaded with different amounts of zein-fibrous clays biohybrids were produced by solution blending. First, a required amount of biohybrid was dispersed in deionized water by vigorous stirring for 24 h at room temperature. Then, the biohybrid suspension was gradually added to the previously prepared 2% (w/v) alginate dispersion in water, in order to achieve alginate:biohybrid mass ratios of 1:1, 1:2, and 1:3, and the mixture was kept under constant stirring overnight. Finally, the resulting bionanocomposites were placed onto a glass plate and allowed to dry at room temperature. The alginate films incorporating zein-sepiolite or zein-palygorskite biohybrid filler were denoted as ALG/Z-SEP# and ALG/Z-PALY#, respectively.

For comparison, pure alginate membranes were produced in the same way from a 2% sodium alginate aqueous solution. After casting onto a glass plate, the resulting dried membranes were in some cases immersed in 5% $CaCl_2$ for 15 min to cross-link the alginate chains. Then, the membranes were washed with doubly distilled water to remove residual Ca^{2+} ions and allowed to dry at room temperature.

Characterization

Viscosity was measured at 25 ± 0.5°C and 100 rpm in a RVDVII+ PRO Brookfield viscometer. Infrared spectra were recorded using samples prepared as self-supporting films by means of attenuated total reflectance mode (ATR-IR) in the Shimadzu GladiATR 10 equipment, or with a FTIR spectrophotometer BRUKER IFS 66v/S. In both cases, the IR spectra were recorded from 4000 to 400 cm^{-1} with 2 cm^{-1} and 4 cm^{-1} of resolution for FTIR and ATR measurements, respectively. CHNS chemical analysis was carried out with a Perkin-Elmer 2400 analyzer. The thermal behavior of the prepared materials was analyzed from the simultaneously recorded thermogravimetric (TG) and differential thermal analysis (DTA) curves in a SEIKO SSC/5200 equipment, in experiments carried out under air atmosphere (flux of 100 mL min^{-1}) from room temperature to 1000°C, at heating rate of 10°C min^{-1}. Surface morphology was observed in FE-SEM equipment FEI-NOVA NANOSEM 230. Sample preparation was performed by adhering particle samples on a carbon tap for direct observation without requirement of any conductive coating on the surface.

Mechanical Properties

Tensile modulus (E) and percentage of elongation at break of the bionanocomposite films were evaluated with a Model 3345 Instron Universal Testing Machine (Instron Engineering Corporation). The elongation was directly determined from the cross-head displacement as the machine was not equipped with an extensometer. The samples were cut (7 cm × 1.5 cm) and mounted between the grips with an initial separation of 50 mm, and the cross-head speed was set a 2 mm min^{-1}. Three replicates were run for each film.

Light Barrier Properties

The film samples were cut into rectangles (1.5 cm x 4 cm) and placed in a special spectrophotometer cell holder for direct evaluation of transmittance. The light barrier properties of the film samples were measured in the transmittance mode at the wavelength interval between 200 and 800 nm, using a UV spectrophotometer (Shimadzu, UV1201 model).

Water Absorption Determination

The polysaccharide-based bionanocomposites were immersed in distilled water at room temperature, and after 24 h the films were withdrawn and the excess of water removed before weighing them on an analytical balance. The water uptake was calculated from the following eq. (1):

$$\text{Water absorption } (g/g) = W_t - W_0/W_0 \quad (1)$$

where W_t and W_0 are the mass of the wet and initial films, respectively.

Gas Permeation

Gas permeation properties of ALG/Z-SEP bionanocomposite membranes were evaluated using the water swollen method. For this purpose, membranes were hydrated in water overnight to form a hydrogel. In order to avoid any disintegration of the membrane in these conditions, these materials were previously

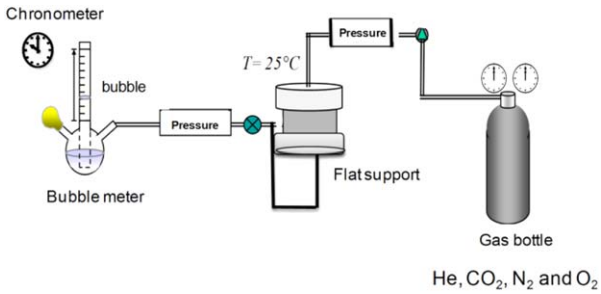

Scheme 1. Experimental set-up for gas permeation testing. [Color figure can be viewed in the online issue, which is available at wileyonlinelibrary.com.]

subjected to a cross-linking process using sodium calcium chloride as cross-linking agent (5% (w/v), 15 min). After hydration, the water excess was removed and the membrane was quickly mounted on a flat permeation support. The permeability of pure gases through the water-swollen hydrogel membranes was determined at different pressures using the constant volume method (Scheme 1). The gas permeability through the membrane was calculated from the following eq. (2):

$$P = Ql/(A \cdot \Delta p) \quad (2)$$

where P is the permeability coefficient of the gas expressed in mol s^{-1} Pa^{-1} m^{-1}, Q the permeate gas flow rate, A the effective membrane area for permeation (17 cm^2), l the membrane thickness and Δp is the pressure difference across the membrane. The thicknesses of the used membranes were between 0.065 and 0.085 mm.

RESULTS AND DISCUSSION

Physicochemical Characterization of the Polysaccharide–Fibrous Clay Bionanocomposites

Previous studies have shown that neutral and charged polysaccharides can interact with the surface of fibrous clay minerals through hydrogen bonding between silanol groups on the clay surface and the hydroxyl, carboxyl or amino groups of the biopolymers, as confirmed in bionanocomposites based on alginate, chitosan, xanthan, starch, and sacran.[12,17,20,21] These interactions with the clay particles can give rise to an increase in the viscosity of the polymer dispersions, similarly as reported in viscosity studies of PVA-clay[33] or in starch, chitosan and alginate based systems involving fibrous clays.[20] In the current work, the viscosity measurements of a set of dispersions of fibrous clays and neutral and negatively charged polysaccharides revealed the pseudoplastic behavior of these preparations. Thus, with the purpose of evaluating the effect of the loaded silicate, the viscosity values were compared at a given shear rate (100 rpm for all the samples) (Figure 2). In general, the viscosity increases in all cases with the increase in the amount of SEP or PALY added to the biopolymer matrix. Among all the tested polysaccharides, the highest viscosity values are obtained for XG and their bionanocomposite dispersions, reaching values around 1600 and 1350 cPs for those dispersions loaded with 50% (w/w) SEP [Figure 2(a)] and 50% (w/w) PALY [Figure 2(b)], respectively.

In SEP-loaded systems, the viscosity values show a considerable growth when 17% (w/w) clay is present in the final composition, reaching values up to 3 times more viscous than the biopolymer alone for those dispersions containing 50% of sepiolite [Figure 2(a)]. In contrast, biopolymer dispersions that incorporate PALY show a more pronounced increase just after the addition of 50% clay in the biopolymer matrix [Figure 2(b)], displaying lower viscosity values compared to the sepiolite systems. As discussed in a previous work, such difference could be attributed to the differences in the rheological properties of the neat clays.[20]

The polysaccharide-fibrous clay bionanocomposites loaded with 33% of sepiolite and the pristine polysaccharides were characterized by IR (Figure 3). The ATR-IR spectra of the polysaccharides [Figure 3(a)] present in all cases a strong vibration band around 1000–1023 cm^{-1}, attributed to C—O stretching vibration corresponding to C—OH groups. Neat PCT and XG spectra [Figure 3(a)] show a vibration band related to ester carbonyl group ($\nu_{C=O}$) at 1735 and 1722 cm^{-1}, respectively,[34] which remains unaltered after sepiolite addition in the biopolymer matrix [Figure 3(b)]. It is also observed in the bionanocomposites spectra [Figure 3(b)] that the band assigned to the asymmetric stretching of —COO^- groups at 1606, 1586, 1593 and 1604 cm^{-1} in the starting PCT, CMC, ALG and XG polysaccharides [Figure 3(a)], respectively, can be overlapped with the

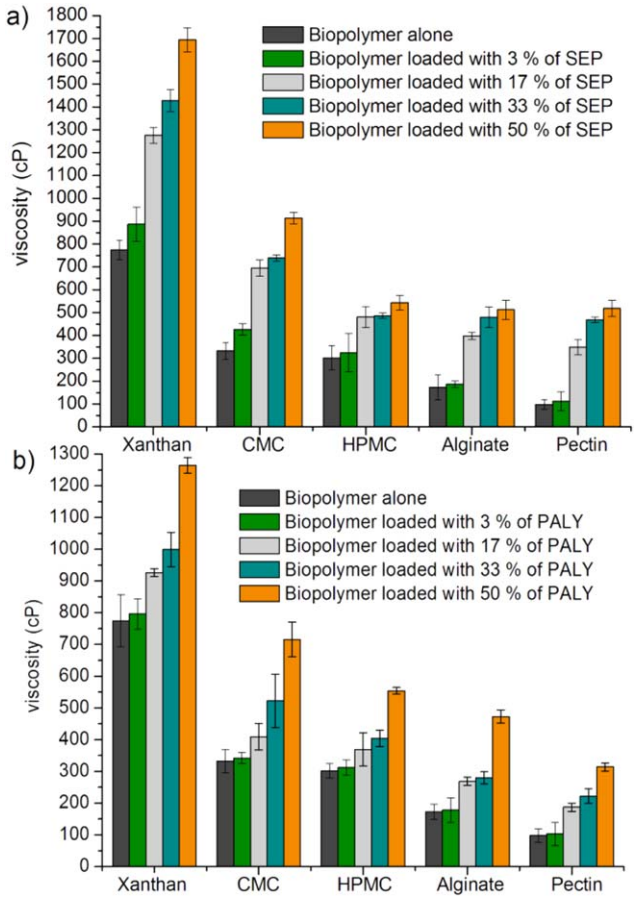

Figure 2. Viscosity values of different polysaccharide solutions (2% (w/v)) and their respective bionanocomposite dispersions (2% (w/v)) based on (a) sepiolite and (b) palygorskite. [Color figure can be viewed in the online issue, which is available at wileyonlinelibrary.com.]

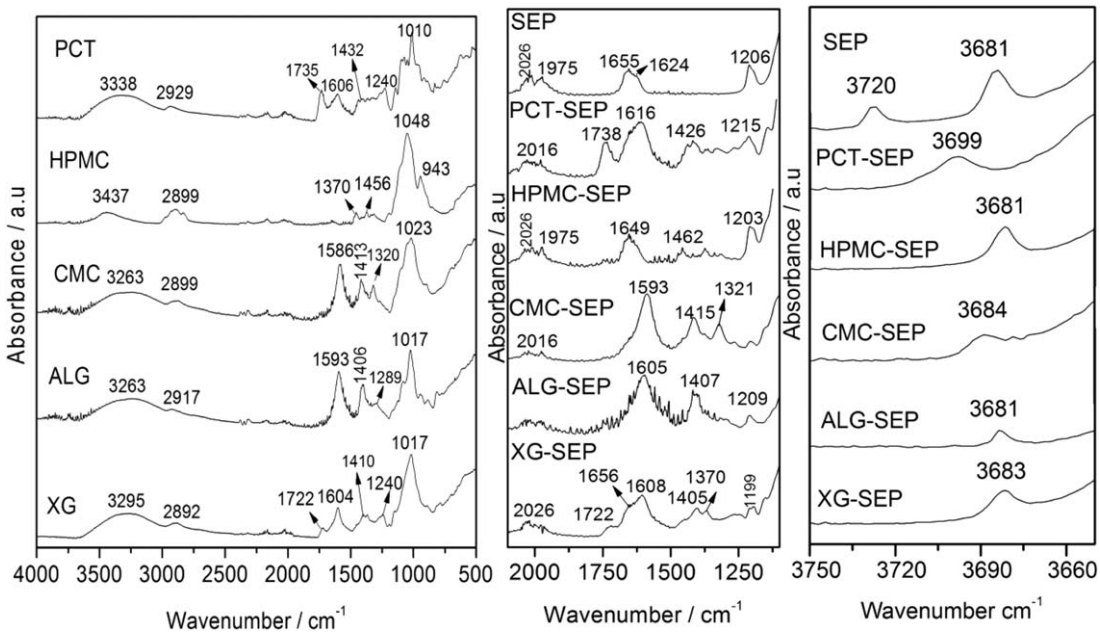

Figure 3. ATR-IR spectra (4000–500 cm^{-1} region) of the (a) starting biopolymers and (b) their respective bionanocomposites loaded with 33% of sepiolite. (c) FTIR spectra (3750-3650 cm^{-1} region) of polysaccharide-sepiolite bionanocomposites.

characteristic bending vibration bands of water molecules (δ_{HOH}) in sepiolite appearing from 1655 to 1624 cm^{-1}. This fact makes very difficult the detection of possible clay-polysaccharides interactions in this region of the spectra. Nevertheless, the carboxyl vibration in pristine PCT and ALG was shifted towards higher wavenumber values, appearing at 1616 and 1605 cm^{-1}, respectively, in the spectra of the derived bionanocomposites [Figure 3(b)], while a shoulder at 1656 cm^{-1} can be appreciated in the spectrum of XG-SEP bionanocomposite, suggesting in these cases a possible interaction between the carboxylate groups ($\nu_{asC=O}$) and the sepiolite. In addition, the bands related to the symmetric stretching vibrations of carboxylate groups ($\nu_{sC=O}$) at 1432 and 1410 cm^{-1} in neat PCT and XG [Figure 3(a)] are also shifted towards lower wavenumber, suggesting interactions between the negatively charged polysaccharides and the clay substrate.

It is noteworthy that, in all the studied systems the band at 3720 cm^{-1}, attributed to the OH stretching vibration of free silanol groups on the external surface of sepiolite, is not appreciable in the spectra of the polysaccharide-clay materials [Figure 3(c)], similarly as observed for analogous systems involving microfibrous clays.[12,15,20,26] This fact is related to the perturbation of the silanols groups in the external surface of sepiolite by interaction through hydrogen bonding with the assembled hydrophilic species, being this band displaced towards lower frequencies and becoming practically inappreciable. Otherwise, the band attributed to the stretching OH vibration of Mg-OH groups at 3681 cm^{-1} located inside the block structure of sepiolite is still observed in the bionanocomposite materials due to the inaccessibility of the biopolymer chains in this zone. These results confirm the establishment of interactions between the polysaccharides and the clay mineral, being the hydroxyl and carboxyl groups present in the polymer backbone involved in such interactions with silanol groups located in the surface of the fibrous clays.

The morphology of the polysaccharide-fibrous clay bionanocomposites was evaluated by means of FE-SEM. As illustrative examples, Figure 4 shows the resulting images of the cellulose derivatives HPMC [Figure 4(a)] and CMC [Figure 4(d)] together with their respective bionanocomposites prepared with 33% (w/w) of SEP [Figure 4(b,e)] or PALY [Figure 4(c,f)]. From these images, it can be confirmed the homogeneity of the bionanocomposite samples and the good integration of the silicate fibers within the polymer matrix, presenting a more compact aspect in the case of the material formed with CMC than HPMC. In this last case, the interaction of both clays with HPMC seems to induce the formation of a layered arrangement, which could be promoted by the deposition of the bionanocomposite dispersion during the processing as film, similarly as reported for chitosan-based bionanocomposites.[12,20]

The thermal stability of the biopolymers CMC and PCT and their respective bionanocomposites loaded with 33% (w/w) SEP was investigated by TG [Figure 5(a,b)] and DTA [Figure 5(a′,b′)]. In both cases, a weight loss around 12% is observed when heating up to 200°C, and it is related to physically adsorbed water molecules. Heating at temperatures higher than 200°C produces various mass loss events for both polysaccharides associated with exothermic processes, as evidenced by DTA curves. Thus, the weight loss around 43% between 200 and 350°C is attributed to the partial decomposition of CMC and PCT, while that associated with exothermic processes in the temperature range 350–800°C can be related to the decomposition of pyrolytic products formed in the incomplete combustion of the polysaccharides at previous stages. Although a

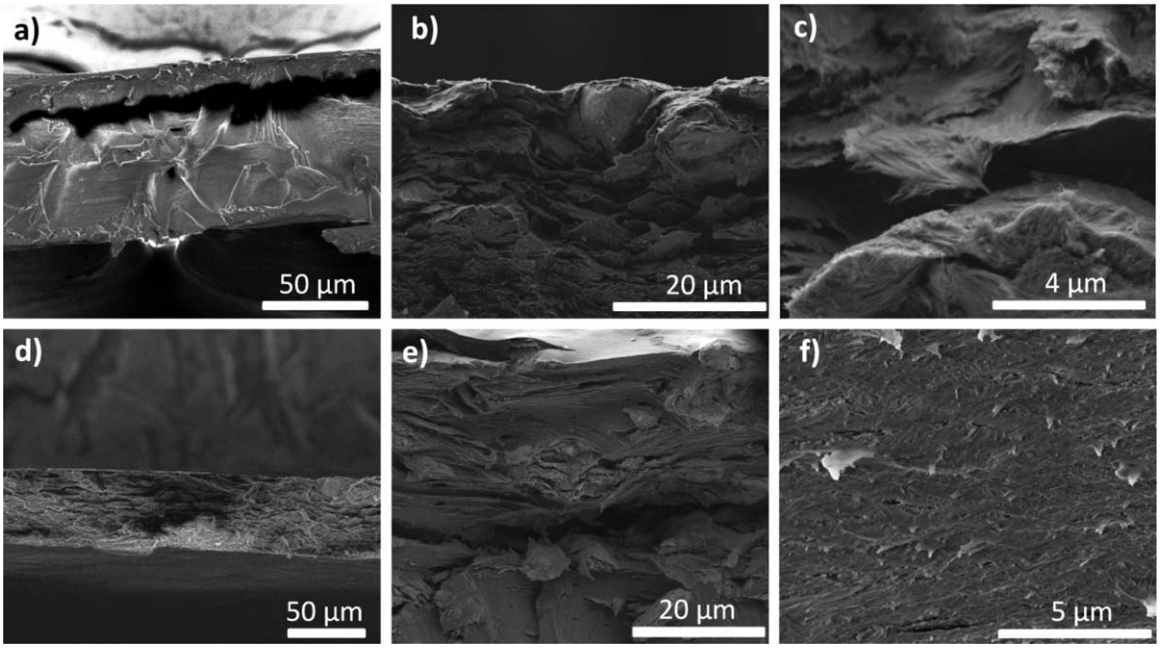

Figure 4. FE-SEM images of the biopolymers HPMC (a) and CMC (d), and their respective bionanocomposites loaded with 33% (w/w) of fibrous clays: HPMC-SEP (b), HPMC-PALY (c), CMC- SEP (e) and CMC-PALY (f).

cooperative behavior between the polysaccharide and SEP can be confirmed by the good thermal stability of the bionanocomposites based on CMC and PCT up to 380 and 465°C, respectively, a clear decrease in the temperatures of decomposition in these hybrid materials can be evidenced. This behavior could be associated with possible changes of the polysaccharide structure when assembled to sepiolite, since pectins and related carbohydrates have a complex structure with helical conformations that could contribute to the improvement of the thermal stability of the native biopolymer, showing oxidation reactions at high temperatures (around 700°C). Similar results were reported in the literature, in studies on the immobilization of pectin into layered double hydroxides.[22]

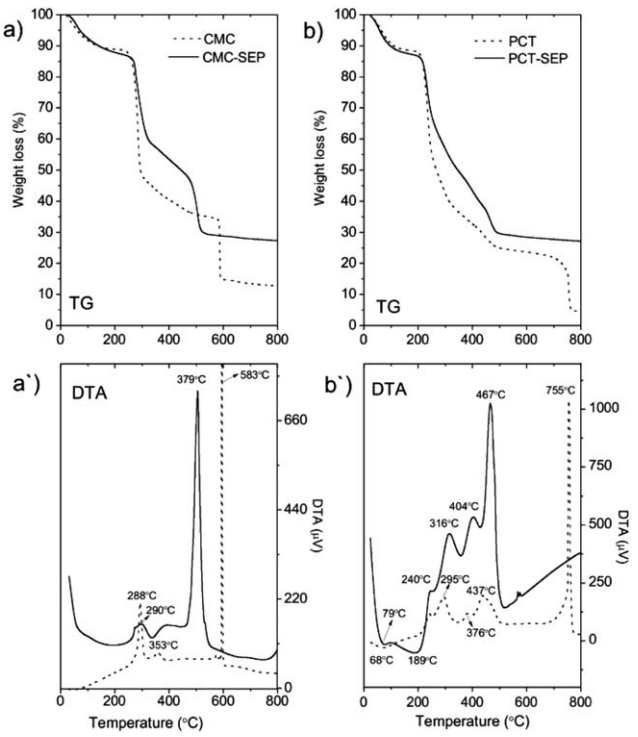

Figure 5. TG (above) and DTA (below) curves recorded in the 25 – 800°C range, under air flow conditions for the bionanocomposites based on CMC (a and a') and PCT (b and b') loaded with 33% (w/w) SEP. In all graphs the dashed lines correspond to both the TG and DTA curves of the pure biopolymer, and the solid lines correspond to TG and DTA of the polysaccharide-sepiolite bionanocomposite.

Effect of the Fibrous Clays on the Physical Properties of the Bionanocomposite Films

The mechanical properties of the bionanocomposites were evaluated as a function of the incorporated amounts of sepiolite and palygorskite in the polysaccharide matrices (Table I). A clear reinforcement effect can be evidenced for those materials loaded with fibrous clays with respect to the unmodified biopolymers, where both tensile modulus and tensile strength increase with the increase of filler amount. In all the studied systems, the tensile strength and Young's moduli of materials incorporating SEP are higher than those loaded with PALY, in accordance with the previously shown viscosity results. This good level of reinforcement in sepiolite-based bionanocomposites could be attributed to the high elastic modulus of single sepiolite crystals,[35] as well as to the high external surface area available in SEP in comparison to PALY for interactions with the polysaccharide chains, as reported for analogous polysaccharides.[20]

As shown in Table I, the CMC bionanocomposite films exhibit the highest Young's modulus values, around 5.94 and 5.23 GPa for the materials CMC/SEP and CMC/PALY, respectively, with a 50% in clay content. It is also remarkable the high increment in

Table I. Tensile Properties of the Different Polysaccharide-Based Bionanocomposites Reinforced With Sepiolite and Palygorskite

	ALG			CMC			HPMC			PCT			XG		
	E (GPa)	Eb (%)	σ (MPa)	E (GPa)	Eb (%)	σ (MPa)	E (GPa)	Eb (%)	σ (MPa)	E (GPa)	Eb (%)	σ (MPa)	E (GPa)	Eb (%)	σ (MPa)
% of SEP	Polysaccharide-sepiolite films														
0	3.88 ± 0.36	6.66 ± 0.78	64.0 ± 17.5	2.83 ± 0.42	4.88 ± 0.89	20.1 ± 3.86	2.38 ± 0.21	4.55 ± 0.16	17.3 ± 3.14	0.87 ± 0.13	2.17 ± 0.22	7.15 ± 1.13	0.82 ± 0.23	2.09 ± 0.23	6.9 ± 1.08
3	4.29 ± 0.32	5.88 ± 0.12	69.3 ± 19.6	4.25 ± 0.32	4.12 ± 0.21	29.7 ± 3.68	3.07 ± 0.12	3.07 ± 0.70	22.4 ± 2.78	2.50 ± 0.10	1.98 ± 0.18	19.8 ± 1.99	1.44 ± 0.38	1.81 ± 0.44	11.9 ± 1.22
17	4.93 ± 0.24	4.19 ± 0.74	80.2 ± 14.9	5.25 ± 0.54	3.30 ± 0.54	38.2 ± 7.19	4.97 ± 0.36	2.82 ± 0.17	33.1 ± 5.94	3.88 ± 0.26	1.76 ± 0.32	31.2 ± 2.76	2.08 ± 0.11	1.78 ± 0.12	17.6 ± 0.97
33	5.10 ± 0.17	3.90 ± 0.19	82.1 ± 18.4	5.85 ± 0.48	2.78 ± 0.32	42.3 ± 9.62	5.44 ± 0.22	2.16 ± 0.11	39.3 ± 6.98	4.40 ± 0.23	1.74 ± 0.15	35.5 ± 2.34	2.28 ± 0.13	1.65 ± 0.29	19.4 ± 1.98
50	5.20 ± 0.12	3.27 ± 0.45	84.2 ± 23.1	5.94 ± 0.36	2.34 ± 0.21	42.9 ± 9.22	5.48 ± 0.14	2.08 ± 0.23	39.8 ± 4.44	4.47 ± 0.32	1.70 ± 0.14	36.0 ± 4.67	2.86 ± 0.38	1.56 ± 0.16	24.2 ± 2.22
% of PALY	Polysaccharide-palygorskite films														
0	3.88 ± 0.36	6.66 ± 0.78	64.0 ± 12.9	2.83 ± 0.42	4.88 ± 0.89	20.1 ± 3.86	2.38 ± 0.21	4.55 ± 0.16	17.3 ± 3.14	0.87 ± 0.13	2.17 ± 0.13	7.15 ± 1.13	0.82 ± 0.23	2.09 ± 0.23	6.9 ± 1.08
3	4.05 ± 0.24	5.73 ± 0.61	66.7 ± 13.2	3.05 ± 0.52	3.83 ± 0.22	21.7 ± 3.33	3.05 ± 0.32	3.00 ± 0.45	22.7 ± 3.98	1.20 ± 0.12	2.08 ± 0.44	9.7 ± 1.04	1.02 ± 0.15	1.88 ± 0.11	8.60 ± 1.22
17	4.24 ± 0.21	4.22 ± 0.11	68.7 ± 18.0	4.68 ± 0.32	3.00 ± 0.17	32.0 ± 5.12	3.95 ± 0.11	2.74 ± 0.21	30.3 ± 4.87	2.22 ± 0.20	1.87 ± 0.16	16.4 ± 3.91	1.85 ± 0.22	1.80 ± 0.17	15.5 ± 0.97
33	4.54 ± 0.56	3.82 ± 0.33	72.3 ± 19.2	4.92 ± 0.12	2.77 ± 0.41	33.5 ± 4.98	4.52 ± 0.10	2.03 ± 0.18	33.3 ± 5.23	2.75 ± 0.41	1.81 ± 0.29	21.3 ± 2.76	2.22 ± 0.20	1.76 ± 0.22	17.9 ± 1.98
50	4.78 ± 0.22	2.13 ± 0.15	78.8 ± 21.1	5.23 ± 0.41	2.09 ± 0.16	36.9 ± 8.09	4.96 ± 0.21	1.98 ± 0.26	35.8 ± 8.74	3.05 ± 0.30	1.82 ± 0.40	24.8 ± 4.44	2.35 ± 0.19	1.64 ± 0.42	19.7 ± 2.22

E = tensile modulus, Eb = elongation at break and σ = tensile strength.

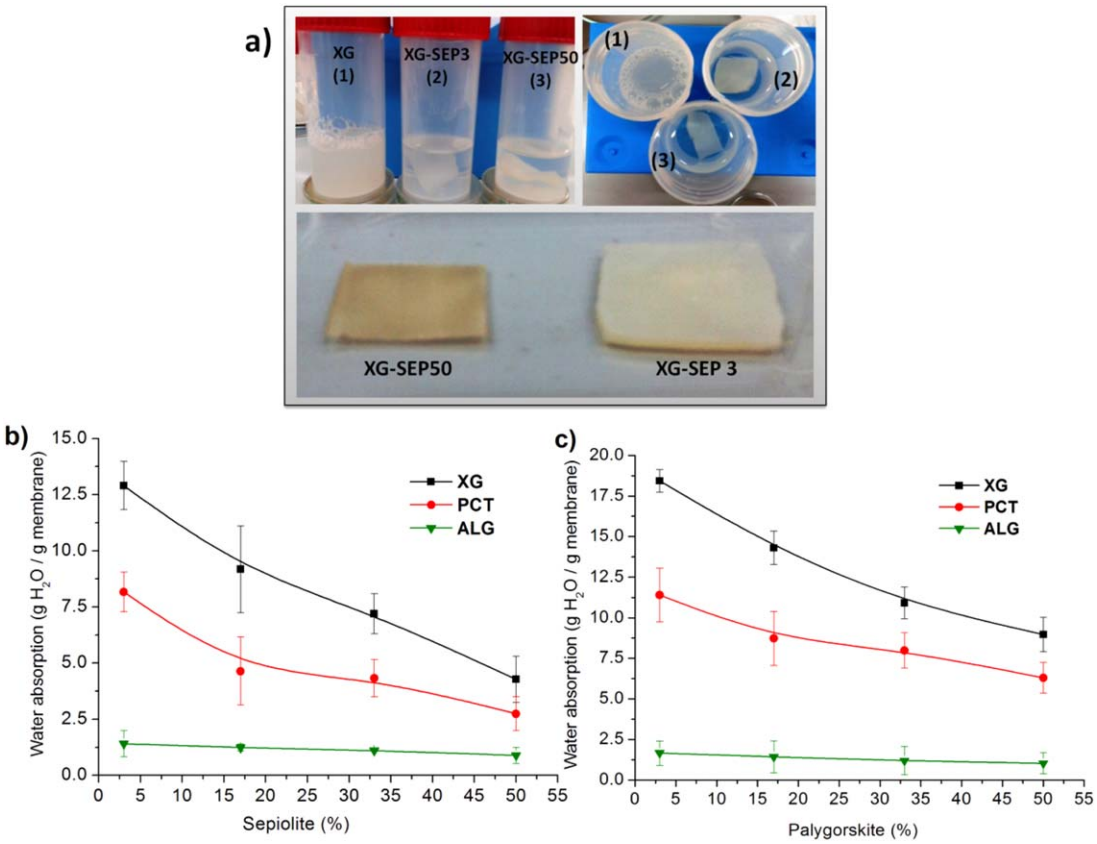

Figure 6. (a) Water resistance and macroscopic appearance of swelled XG unmodified films (1) and their bionanocomposite films loaded with 3% (2) and 50% (w/w) (3) of sepiolite filler after water absorption assay. Effect of (b) SEP and (c) PALY on the water absorption of polysaccharide films containing different amounts of filler. Measures performed in deionized water (pH 5.5). [Color figure can be viewed in the online issue, which is available at wileyonlinelibrary.com.]

the tensile modulus of pectin after the addition of sepiolite, increasing from 0.87 GPa to 4.47 GPa with a 50% sepiolite loading. Conversely to the typical behavior of analogous nanocomposite materials based on layered clays, where mechanical properties are just improved at low clay loadings (approx. up to 7%),[36] the bionanocomposites prepared employing fibrous clays as filler, show an increase in Young's modulus with the increase of the clays content, even at high filler loadings [50% (w/w)]. This interesting behavior in bionanocomposite materials based on fibrous clays was already observed by other authors,[12,13,20,37,38] being attributed to the strong interactions at the nanometer range between both components in fibrous clays-reinforced biopolymer materials. This high degree of interaction between the silicate fibers and the polysaccharide chains was also suggested by the high viscosity values of the bionanocomposite dispersions containing fibrous clays compared with the pristine biopolymer (Figure 2). In contrast, elongation-at-break values of the polysaccharide-clay films are decreased with respect to the value measured for the neat biopolymer film, indicating a reduction in the plastic behavior of all the bionanocomposite films. Such a decrease can be attributed to the reduced mobility of the biopolymer chains after their assembling to the clay fibrils as discussed above.

As previously reported for analogous systems,[20] these strong polysaccharide-fibrous clay interactions can also reduce the water uptake ability in the resulting materials, due to the decrease of the available OH groups in the polysaccharide chains, increasing their stability in aqueous media. In fact, the contact of non-modified polysaccharides with water provokes a fast swelling of the film and leads to their disintegration, making it impossible to determine their water uptake capacity [Figure 6(a-1)]. In contrast, the assembly of SEP and PALY to these polysaccharides significantly improves their water resistance due to their effect as physical crosslinking agents, analogously to that reported for montmorillonite sheets in a guar gum matrix,[39] and the resulting films can maintain their integrity during and after the assay [Figure 6(a-2) and (a-3)]. Water absorption (pH 5.5) of the bionanocomposites as a function of the clay content is displayed in Figure 6(b,c). The water absorption is influenced in all cases by the clay content, showing a decrease of the water uptake as the filler loading increases. This fact is remarkable in the case of XG-based bionanocomposites, which showed a significant reduction of the water absorption values when the clay content increases from 3% to 17%, with decreases around 25% and 22% in SEP-loaded [Figure 6(b)] and PALY-loaded materials, respectively [Figure 6(c)]. These values were further reduced around 65% and 50% when the SEP

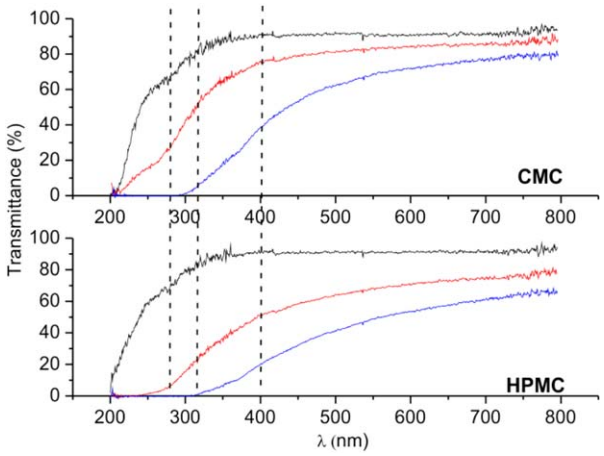

Figure 7. Transmittance measurements in the 200–800 nm wavelength interval of CMC and HPMC bionanocomposite films prepared with different loadings of SEP: 0 (black line, upper line), 17% (w/w) (red line, middle line) and 33% (w/w) (blue line, lower line). [Color figure can be viewed in the online issue, which is available at wileyonlinelibrary.com.]

and PALY content reached 50% (w/w) in the XG matrix, respectively. Similar behavior is observed for PCT-based bionanocomposite films, where a clear decrease of the water uptake upon addition of 17% of SEP or PALY in the biopolymer matrix can be evidenced. These values become almost constant up to 33% of added clay, decreasing once again at higher clay concentrations (50% w/w). On the other hand, bionanocomposite films based on ALG exhibit good stability in water, although the water absorption remains practically constant at clay loadings higher than 17% (w/w).

The light barrier properties of the bionanocomposite films that incorporate SEP as filler were evaluated by measuring transmittance values in a wavelength range between 200 and 800 nm, as illustrated in Figure 7 with the results obtained for CMC and HPMC-based systems. The samples exhibited reduced light transmission in the UV region, in comparison to the pure polysaccharide films. For instance, HPMC-based bionanocomposite films show a decrease in the transmittance in the visible region as the filler content increases, being reduced for instance from 92% in the neat HPMC film to 72% and 54% at 600 nm when the sepiolite loading is 17% (w/w) and 33% (w/w), respectively. A noteworthy barrier towards UV light is evidenced, reaching practically null values of transmittance for the HPMC films incorporating 33% (w/w) of sepiolite at wavelengths below 300 nm. These results suggest a well dispersion of the filler particles within the biopolymer matrix, providing enough transparency but acting at the same time as a barrier to block the UV radiation. Thus, these reinforced biopolymer films can be potentially applied for food protection because they are able to inhibit the passage of UV light, similarly to reported alginate films loaded with ginseng extract as an antioxidant bioadditive.[40]

Effect of Zein-Modified Fibrous Clays on the Physical Properties of Alginate Films

As shown in the previous section, fibrous clay-loaded alginate films offer improved mechanical properties, but the water uptake is only slightly reduced with respect to the neat polysaccharide. Thus, the use of the filler modified with hydrophobic compounds of biological origin instead of common organoclays could contribute to enhance the water resistance of alginate-based bionanocomposite films, preserving the green character of the bioplastics. In this context, the assembly of the corn protein zein to sepiolite and palygorskite was reported by Alcântara *et al.*,[15] showing the ability of this protein to reduce the hydrophilic character of these fibrous clays, which allows to consider the resulting bio-organoclays as alternative ecological fillers in the development of plastics for food packaging. Those previous tests showed an improvement of the plastic behavior in alginate matrices loaded with both Z-SEP and Z-PALY biohybrids, with an increase in the elongation at break values up to values around 20%, which was attributed to the plasticizing effect of zein. According to Wang *et al.*,[41] this protein has a high affinity towards carboxylic groups, being the interactions between available functional groups of zein and carboxylic groups of alginate critical to reach zein plasticization. This effect was accompanied by a slight reduction of the Young's modulus of pristine alginate (3.9 GPa) upon addition of zein-clay biohybrids, reaching values ranging between 3.79 and 1.00 GPa depending on the amount of loaded biohybrid as well as the amount of zein assembled to the clay.[15]

The use of nanofillers in which sepiolite and palygorskite are previously modified with this hydrophobic protein can provide the resulting bionanocomposites with different properties, in comparison with those materials loaded with unmodified fibrous clays. For instance, contact angle (θ) values were determined in alginate-based bionanocomposite films in order to determine the hydrophobic or hydrophilic characteristics of their surface, and they are summarized in Table II. A quantitative definition of the relative terms hydrophobic and hydrophilic surfaces has been done for surfaces exhibiting water contact angles higher than 65° and lower than 65°, respectively.[42] In the case of the zein-clay loaded bionanocomposites, all the films here analyzed showed hydrophobic surfaces with very close contact angle values between 81° and 88° (Table II). In contrast, films of alginate loaded with neat sepiolite show the less hydrophobic values, showing a decrease in the contact angle to a value close to 67°. This significant increase in the contact angle in comparison to the alginate-sepiolite film may be related to the reduced hydrophilicity showed by sepiolite fibers once assembled to zein protein, providing these alginate-biohybrid films with a higher hydrophobic surface than the alginate films loaded only with pristine sepiolite. Pure alginate film shows a

Table II. Contact Angles of Water on Alginate Films Loaded with Sepiolite and Z-SEP Biohybrids in 1:1 Alginate:Filler Ratio

Sample	Contac angle (degree)
ALG	90.4 ± 20.08
ALG/SEP	67.1 ± 15.33
ALG/Z-SEP10	88.2 ± 4.95
ALG/Z-SEP29	81.3 ± 2.17
ALG/Z-SEP48	84.3 ± 5.13

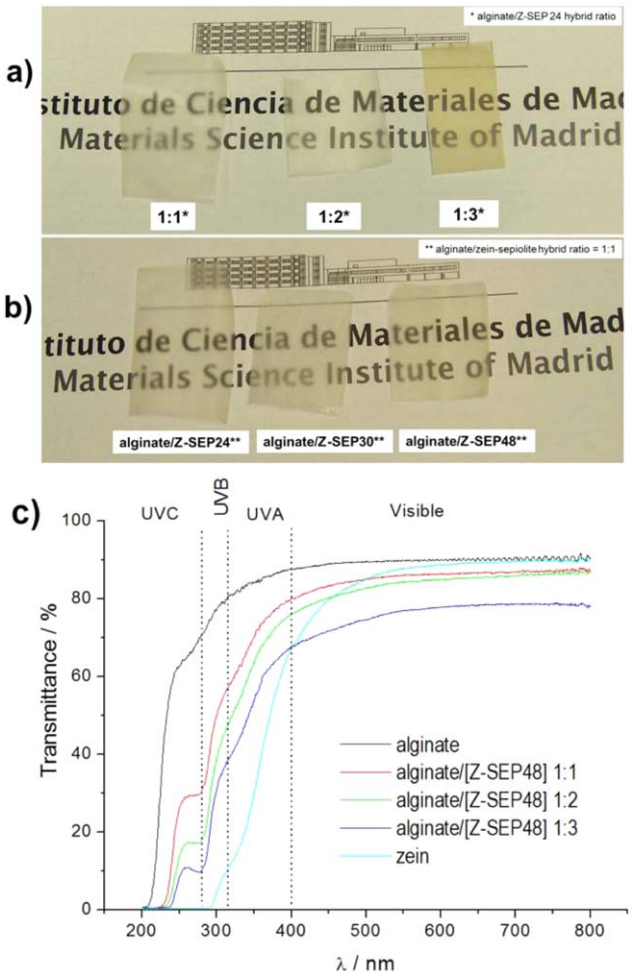

Figure 8. Macroscopic appearance of various bionanocomposite films based on (a) ALG/Z-SEP24 biohybrid prepared with 1:1, 1:2 and 1:3 alginate:biohybrid mass ratios and (b) bionanocomposite films with a fixed 1:1 alginate:biohybrid ratio based on Z-SEP biohybrids of different zein content. (c) Transmittance measurements in the 200–800 nm wavelength range of films of pure alginate, pure zein and ALG/Z-SEP48 bionanocomposites with different alginate:biohybrid ratio. [Color figure can be viewed in the online issue, which is available at wileyonlinelibrary.com.]

value around 90°, which may be related to its high crystallinity, leading to the slow diffusion of water from the outside to the inside of the film.

The water contact angle results are in agreement with previous studies carried out on these materials regarding their water uptake ability and water vapor transmission rate (WVTR).[15] In fact, the maximum water uptake of around 1.2 g of water per g of alginate was only reduced to 0.9 g g^{-1} when neat sepiolite was used as filler (in 1:1 ratio), but the use of zein-clay nanofillers increased the water resistance of the bionanocomposite films. Thus, values of 0.54 and 0.80 g of water per g of film were obtained for alginate films containing Z-SEP48 and Z-PALY28 bio-organoclays in 1:1 mass ratio, respectively. The water uptake properties could be also modified by increasing the amount of added bio-organoclay, reaching values around 0.75, 0.64, and 0.47 g of water per g of film for the ALG/Z-SEP24 samples prepared in 1:1, 1:2 and 1:3 alginate:biohybrid mass ratio, respectively. Similarly, it was confirmed the enhancement of the water vapor barrier properties of alginate films involving zein-modified clays as fillers.[15] Thus, the WVTR of neat alginate films (1.14 mg h^{-1} cm^{-2}) was only reduced to 0.88 mg h^{-1} cm^{-2} in 1:1 ratio ALG:SEP films, but it showed a huge reduction when zein-loaded clays were used as fillers instead of pristine clays, reaching values of 0.29, 0.20, and 0.17 mg h^{-1} cm^{-2} for the ALG/Z-SEP48 samples prepared in 1:1, 1:2 and 1:3 alginate:biohybrid mass ratio, respectively. All these results suggest a significant compatibility between the zein-based biohybrids and the alginate matrix as the films become more stable and water resistant than pure alginate and alginate-SEP films, being so a promising alternative as bioplastic for applications in food packaging. Actually, the possibility to modulate water-uptake properties of zein-alginate systems was used in the development of beads for controlled drug delivery in aqueous media.[43]

Besides the improved water barrier properties, the resulting self-standing films loaded with zein-fibrous clay biohybrids show considerable homogeneity and transparency, independently of the amount [Figure 8(a)] and the type [Figure 8(b)] of biohybrid incorporated in the alginate matrix. The small differences observed amongst bionanocomposite films can be associated with differences in their thickness. Light barrier properties of these bionanocomposite films were evaluated by measuring transmittance values in a wavelength range between 200 and 800 nm. From the data represented in Figure 8(c), it is clear that all the tested films exhibit reduced light transmission in the UV region, compared to the pure alginate films. When the bio-organoclay content in the alginate matrix increases, a decrease in the transmittance occurs. Transmittance in the UV region may decrease till around 10% in alginate films incorporating the Z-SEP48 sample in a 1:3 alginate:biohybrid ratio, which is the sample with the highest content in biohybrid, and so in zein. These results suggest a good dispersion of the biohybrid particles within the alginate matrix, acting as a good barrier to prevent the passage of UV light. Thus, it can be concluded that zein-based organoclays can also play a role as additive of alginate films affording good transmittance in the visible region but inhibiting the passage of UV light, which can be of interest in view to a potential application in food protection, similarly to ginseng extract used as an antioxidant bio-additive that additionally impart light barrier properties to the alginate films.[40]

Gas barrier properties are also important regarding the application of bioplastics in food packaging. Similarly to other hydrophilic polymeric membranes, alginate films show low gas permeation property in dry state, but in wet conditions their permeability values increase substantially,[44] being a disadvantageous feature in the food packaging sector. Therefore, gas barrier properties of alginate films were also evaluated in wet conditions, focusing on films loaded with zein-sepiolite biohybrids as they showed the best water resistance properties. For this purpose, films were previously cross-linked with Ca^{2+} ions, swollen in water overnight and then permeabilities of pure gases through these wet membranes were evaluated as detailed in the

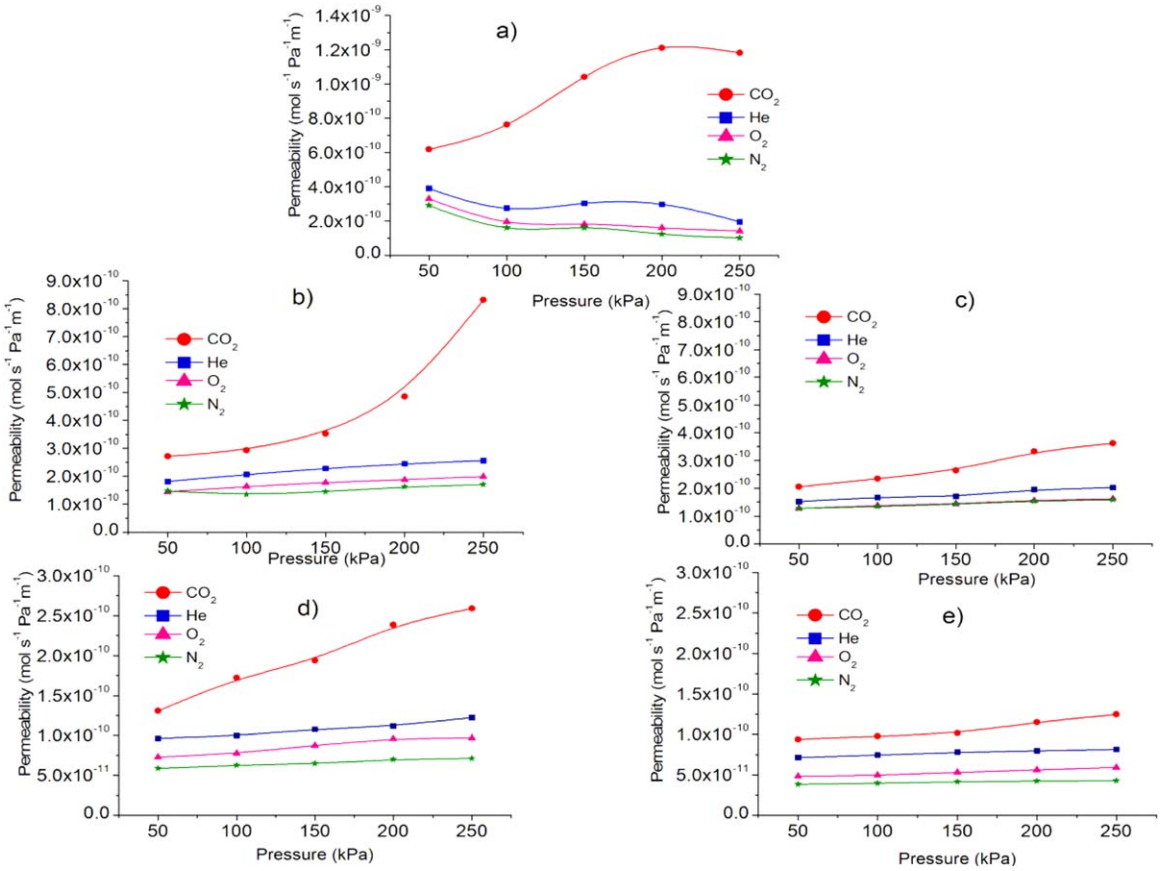

Figure 9. Gas permeation properties of wetted membranes cross-linked with Ca^{2+} ions, based on pure alginate (a), as well as on ALG/Z-SEP16 (b and c) and ALG/Z-SEP 24 (d and e) bionanocomposites in a 1:1 and 1:2 alginate:biohybrid ratio, respectively. [Color figure can be viewed in the online issue, which is available at wileyonlinelibrary.com.]

Experimental section. Firstly, the water uptake properties of the cross-linked membranes were evaluated, being observed that all them become more stable after the cross-linking process (Table III). The cross-linking with Ca^{2+} ions seems to be less effective in the bionanocomposite membranes compared to that based on the pure alginate film, which is now able to preserve its integrity even after 24 h. This behavior can be attributed to the fact that in the bionanocomposite membranes many of the carboxylic groups of the alginate available for the cross-linking process with calcium cations are already blocked due to their interaction with zein, as discussed above. Here again, it is observed a decrease in water absorption with the increase of the zein in the sepiolite biohybrid and with the biohybrid content in the polysaccharide matrix, which is in accordance with the hydrophobic efficiency introduced by the zein present in the biohybrid.

The permeability of the bionanocomposite membranes towards different gases, such as He, O_2 and CO_2, was first tested in dry state, showing a very low permeability under such conditions, which is good for their application as bioplastics. Taking advantage of the high stability in water of these films, we studied then the gas permeation (CO_2, O_2, He and N_2) in wet membranes because in certain applications the bioplastics could be in contact with moisture and so their gas permeation properties could change. The permeability of CO_2, O_2, He, and N_2 through wetted membranes of pure alginate and alginate loaded with Z-SEP16 and ZSEP24 bioorganoclays in a 1:1 and 1:2 alginate:biohybrid ratio was determined (Figure 9). In general, all the membranes show a pronounced permeability towards CO_2

Table III. Water Uptake of Membranes Based on Pure Alginate and on Alginate Loaded with Z-SEP16 and Z-SEP24 Biohybrids, in Both Cases before and after the Cross-Linking Process

	Water uptake (g H_2O/g membrane)	
Sample	Uncross-linked membranes	Cross-linked membranes with Ca^{2+}
ALG	–[b]	2.75 ± 0.33
ALG/Z-SEP16 (1:1)[a]	0.90 ± 0.19	0.84 ± 0.15
ALG/Z-SEP16 (1:2)[a]	0.82 ± 0.12	0.70 ± 0.12
ALG/Z-SEP24 (1:1)[a]	0.75 ± 0.11	0.68 ± 0.17
ALG/Z-SEP24 (1:2)[a]	0.64 ± 0.09	0.52 ± 0.09

[a] The values correspond to the alginate:biohybrid mass ratio;
[b] the membrane disintegrates by exposure to water.

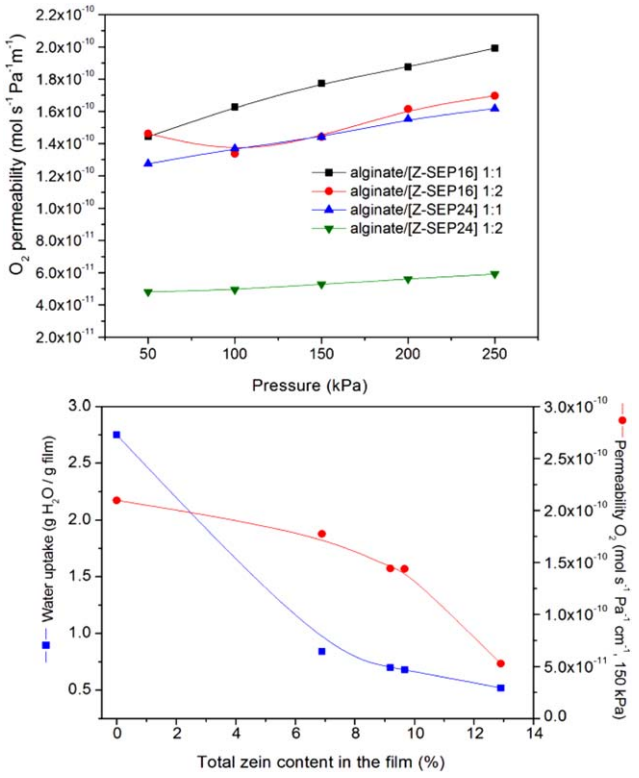

Figure 10. Oxygen permeation of the wetted bionanocomposite membranes (a) and evolution of water uptake values and O_2 permeability as a function of zein content in ALG-ZSEP bionanocomposite membranes (b). [Color figure can be viewed in the online issue, which is available at wileyonlinelibrary.com.]

compared to the other tested gases. Pure alginate film [Figure 9(a)] shows an increase in the CO_2 permeability when the gas pressure increases, while the permeability slightly decreases with pressure in the case of He, O_2 and N_2. Similar trends toward carbon dioxide permeation in water swollen membranes were observed in other studies reported in the literature, although the permeability values found here for alginate membranes are considerably higher compared to those found on diverse hydrogel membranes based on alginic acid or chitosan.[44–46] This behavior can be explained considering the high solubility of acid gases, such as CO_2 in water, which may facilitate the passage of this type of gas through the wetted membranes by increasing its concentration inside the membrane.[45] In contrast, solubility of He, O_2, and N_2 in water is lower than CO_2, because they have weaker interactions with water molecules and therefore the effect results in a lower permeability of these gases when pressure increases.[47,48] According to various studies reported in the literature, which have qualitatively analyzed the state of water in cellulose-type membrane, it was concluded that these polysaccharide-based membranes have a certain degree of molecular order which controls the water entering to the membrane affecting to CO_2 passage but not too much to other gases permeability.[49,50] In the same way than WVTR measurements, the permeabilities towards the same gases in the bionanocomposites membranes decrease significantly and depend on the incorporated type and the amount of the biohybrid, being in all cases lower than those measured for membranes based on pure alginate [Figure 9(b,e)]. The decrease in the permeability values is more marked when the membrane incorporates higher amounts of biohybrid, i.e., the involved membrane presents a lower content in water. The fact that the increase in the permeability of carbon dioxide with the gas pressure was more effective in the membranes loaded with Z-SEP16 [Figure 9(b,c)] than with Z-SEP24 [Figure 9(d,e)] can be related to the higher water content in the first ones, which favors CO_2 solubilization. Conversely to that observed in membranes of pure alginate, the bionanocomposite membranes show a slight increase in the permeability of He, O_2, and N_2 gases as the gas pressure increases, being the coefficients of permeability of He, O_2, and N_2, in the later lower than those found for the alginate membrane. These results indicate the existence of a gas barrier effect of the biohybrid present in the bionanocomposite films which does not seem to influence only in the water content because the amount and type of biohybrid used as nanofiller contributes also to difficult the passage of the gases. Thus, the increase in the barrier properties in ALG/Z-SEP bionanocomposite materials can be attributed to the tortuous path for gas diffusion due to the biohybrid particles distributed in the polysaccharide matrix, consequently increasing the effective diffusion path length as occurs in other polymer-clay nanocomposites. Furthermore, the good dispersion of the biohybrid within the biopolymer matrix may result in a lower free volume between polymer chains and filler, improving therefore the barrier properties under humid conditions.

Oxygen permeability is crucial in bioplastics for food packaging applications. As commented above, the O_2 permeability of the prepared bionanocomposite films increases with the pressure, and at the same time it decreases depending on the amount and type (Z-SEP16 or Z-SEP24) of the incorporated nanofiller [Figure 10(a)]. Thus, the film loaded with Z-SEP16 biohybrid in the 1:1 alginate:biohybrid ratio mass shows higher O_2 permeability values than the alginate films with Z-SEP24 in the same ratio. In both systems, a decrease in the permeability values is measured when the amount of biohybrid is increased to a 1:2 alginate:biohybrid mass ratio. In this sense, a marked barrier effect was demonstrated for the ALG/Z-SEP24 film in the 1:2 ratio, which presents O_2 permeability almost constant with increasing pressure, reaching values below 5.0 x 10^{-11} mol s^{-1} Pa^{-1} m^{-1}. From these results, it is clear the contribution of zein to the observed behavior towards the passage of gases in bionanocomposite membranes. This effect can be better ascertained by analyzing the variation of the O_2 permeability and water uptake of the film with respect to the percentage of zein present in the bionanocomposite material [Figure 10(b)]. Although the presence of the protein limits the indiscriminate entry of water molecules, this behavior does not strongly affect the oxygen permeabilities until the total zein fraction in the film reaches values of 10%. However, for higher contents of zein the permeability toward O_2 is significantly reduced. These results suggest that bionanocomposite films of alginate loaded with Z-SEP biohybrids can be effective against oxygen even under high humidity conditions, which is an advantageous feature that would allow the application of these materials in the

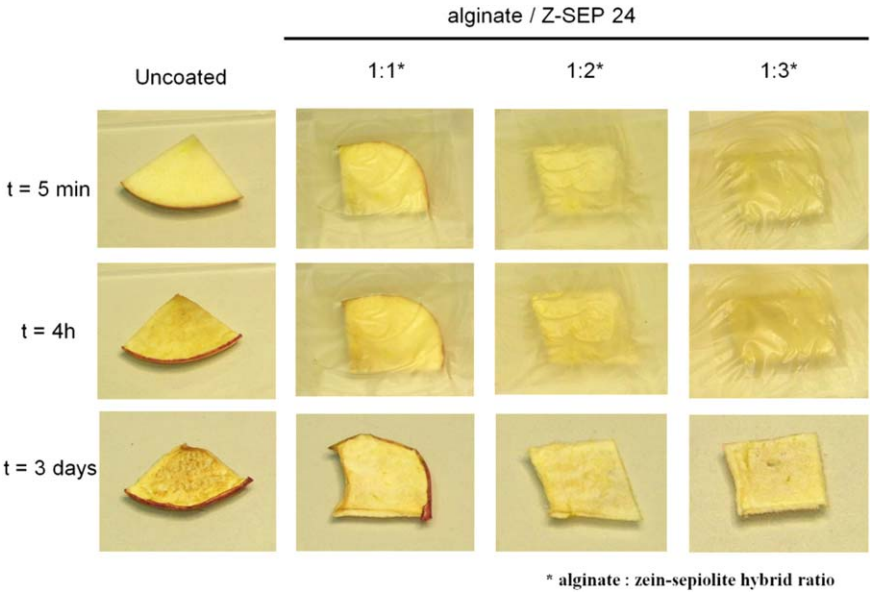

Figure 11. Evaluation of the protective role of various ALG/[Z-SEP24] bionanocomposite films against oxidation of apple slices. [Color figure can be viewed in the online issue, which is available at wileyonlinelibrary.com.]

food packaging sector. Actually, the protection effect of these bionanocomposite films against oxidation of food was proved by a simple test consisting in the observation of the aspect of apple slices after being coated with films loaded with different content in Z-SEP24 (i.e., different zein content) at various periods of time (Figure 11). In accordance to the results discussed above, the membrane with the highest content in zein (1:3 alginate:biohybrid ratio) shows the best barrier properties to the passage of oxygen, preventing the oxidation of the fruit slice even after 3 days. This result yields a simple verification of the good barrier properties of the ALG/Z-clay bionanocomposites towards the passage of water vapor and oxygen, being so promising materials for packaging applications in the food area.

CONCLUSIONS

The use of sepiolite and palygorskite fibrous clays as reinforcing filler in several neutral or negatively charged polysaccharides matrices is here reported. The hydroxyl and carboxyl groups of the polysaccharide chains strongly interact with the surface of the fibrous clays. Hydrogen bonding between the OH groups of the biopolymers and the silanol groups located at the external surface of the fibrous silicates is probably the main interaction mechanism giving rise to highly stable bionanocomposites. The good compatibility between the biopolymers and the fibrous clays resulted in good mechanical properties, improved stability in water and reduction of water absorption, which together with their enhanced barrier to UV light, make these bionanocomposites very attractive as bioplastics in the food packaging sector. Fibrous clays modified with the hydrophobic protein zein were also tested as fillers in one of these polysaccharide matrices, alginate. The assembling of zein reduces the hydrophilic character of the pristine clays, conferring new properties to the resulting biohybrid fillers. The alginate/zein-clay systems are able to form self-supporting films that show a marked resistance to the passage of water molecules in comparison to films of neat alginate or alginate loaded with the pristine clays. The presence of zein assembled to the clay fibers has a crucial role in the water vapour barrier and gas permeation properties of the alginate films, reducing considerably the water uptake and decreasing the gas permeability even at high humidity conditions. Indeed, the bionanocomposite films prepared here, present homogeneity, transparency, as well as improved barrier properties, being therefore promising as ecofriendly materials with potential applications in food packaging.

ACKNOWLEDGMENTS

This work was supported by the CICYT, Spain (project MAT2012–31759) and the EU COST Action MP1202. The authors thank Mr A. Valera and Mr C. Sebastián for technical assistance in the FESEM-EDX studies.

REFERENCES

1. Tharanathan, R. N. *Trends Food Sci. Tech.* **2003**, *14*, 71.
2. Peelman, N.; Ragaert, P.; De Meulenaer, B.; Adons, D.; Peeters, R.; Cardon, L.; Van Impe, F.; Devlieghere, F. *Trends Food Sci. Tech.* **2013**, *32*, 128.
3. Chivrac, F.; Pollet, E.; Avérous, L. *Mater. Sci. Eng. R* **2009**, *67*, 1.
4. Ruiz-Hitzky, E.; Darder, M.; Fernandes, F. M.; Wicklein, B.; Alcântara, A. C. S.; Aranda, P. *Prog. Polym. Sci.* **2013**, *38*, 1392.
5. Rhim, J. W.; Ng, P. K. W. *Crit. Rev. Food Sci. Nutr.* **2007**, *47*, 411.
6. Rhim, J. W. *Food Sci. Biotechnol.* **2007**, *16*, 691.
7. Xie, F.; Pollet, E.; Halley, P. J.; Avérous, L. *Prog. Polym. Sci.* **2013**, *38*, 1590.

8. Rhim, J.-W.; Park, H.-M.; Ha, C.-S. *Prog. Polym. Sci.* **2013**, *38*, 1629.
9. Youssef, A. M. *Polym.-Plast. Technol.* **2013**, *52*, 635.
10. Guan, Y.; Zhang, B.; Tan, X.; Qi, X.-M.; Bian, J.; Peng, F.; Sun, R.-C. *ACS Sustain. Chem. Eng.* **2014**, *2*, 1811.
11. Chen, X.; Gao, H.; Ploehn, H. J. *Carbohydr. Polym.* **2014**, *101*, 565.
12. Darder, M.; Lopez-Blanco, M.; Aranda, P.; Aznar, A. J.; Bravo, J.; Ruiz-Hitzky, E. *Chem. Mater.* **2006**, *18*, 1602.
13. Chivrac, F.; Pollet, E.; Schmutz, M.; Averous, L. *Carbohydr. Polym.* **2010**, *80*, 145.
14. Fernandes, F. M.; Darder, M.; Ruiz, A. I.; Aranda, P.; Ruiz-Hitzky, E. In Nanocomposites With Biodegradable Polymers. Synthesis, Properties, and Future Perspectives; Mittal, V., Ed.; Oxford University Press: New York, **2011**, Chapter 9, p 209.
15. Alcântara, A. C. S.; Darder, M.; Aranda, P.; Ruiz Hitzky, E. *Eur. J. Inorg. Chem.* **2012**, *2012*, 5216.
16. Ruiz-Hitzky, E.; Aranda, P.; Darder, M.; Fernandes, F. M. In Handbook of Clay Science. Part A: Fundamentals; Bergaya, F.; Lagaly, G., Eds.; Elsevier: Amsterdam & Oxford: **2013**; Chapter 13.3, p 721.
17. Alcântara, A. C. S.; Darder, M.; Aranda, P.; Tateyama, S.; Okajima, M. K.; Kaneko, T.; Ogawa, M.; Ruiz-Hitzky, E. *J. Mater. Chem. A* **2014**, *2*, 1391.
18. Brauner, K.; Pressinger, A. *Miner. Petrol.* **1956**, *6*, 120.
19. Bradley, W. F. *Am. Mineral.* **1940**, *25*, 405.
20. Alcântara, A. C. S.; Darder, M.; Aranda, P.; Ruiz-Hitzky, E. *Appl. Clay Sci.* **2014**, *96*, 2.
21. Ruiz-Hitzky, E.; Darder, M.; Aranda, P.; Martin del Burgo, M. Á.; del Real, G. *Adv. Mater.* **2009**, *21*, 4167.
22. Darder, M.; Lopez-Blanco, M.; Aranda, P.; Leroux, F.; Ruiz-Hitzky, E. *Chem. Mater.* **2005**, *17*, 1969.
23. Ruiz-Hitzky, E.; Ariga, K.; Lvov, Y. M. Bio-inorganic Hybrid Nanomaterials, Strategies, Syntheses, Characterization and Applications; Wiley-VCH: Weinheim, **2008**.
24. Ruiz-Hitzky, E.; Aranda, P.; Darder, M.; Rytwo, G. *J. Mater. Chem.* **2010**, *20*, 9306.
25. Ruiz-Hitzky, E. In Functional Hybrid Materials; Gómez-Romero, P.; Sanchez, C., Eds.; Wiley-VCH: Weinheim, **2004**; Chapter 2, p 15.
26. Wicklein, B.; Darder, M.; Aranda, P.; Ruiz-Hitzky, E. *ACS Appl. Mater. Int.* **2011**, *3*, 4339.
27. Wicklein, B.; Darder, M.; Aranda, P.; Ruiz-Hitzky, E. *Langmuir* **2010**, *26*, 5217.
28. Takahashi, H.; Yamada, K.; Yanai, N. U.S. Pat. 5,585,060, **1996**.
29. Bai, J.; Alleyne, V.; Hagenmaier, R. D.; Mattheis, J. P.; Baldwin, E. A. *Postharvest Biol. Technol.* **2003**, *28*, 259.
30. Padua, G. W.; M., R. A.; Ha, T. T., U.S. Pat. 20040056388 A1, **2004**.
31. Gáspár, M.; Benkő, Z.; Dogossy, G.; Réczey, K.; Czigány, T. *Polym. Degrad. Stab.* **2005**, *90*, 563.
32. Ghanbarzadeh, B.; Oromiehi, A. R. *Int. J. Biol. Macromol.* **2008**, *43*, 209.
33. Ristolainen, N.; Heikkilä, P.; Harlin, A.; Seppälä, J. *Macromol. Mater. Eng.* **2006**, *291*, 114.
34. Filippov, M. P. *J. Appl. Spectrosc.* **1972**, *17*, 1052.
35. Fernandes, F. M.; Vazquez, L.; Ruiz-Hitzky, E.; Carnicero, A.; Castro, M. *RSC Adv.* **2014**, *4*, 11225.
36. Rhim, J.-W. *Carbohydr. Polym.* **2011**, *86*, 691.
37. Fernandes, F. M.; Ruiz, A. I.; Darder, M.; Aranda, P.; Ruiz-Hitzky, E. *J. Nanosci. Nanotechnol.* **2009**, *9*, 221.
38. Fukushima, K.; Tabuani, D.; Abbate, C.; Arena, M.; Ferreri, L. *Polym. Degrad. Stab.* **2010**, *95*, 2049.
39. Branca, C.; Crupi, C.; D'Angelo, G.; Khouzami, K.; Rifici, S.; Visco, A.; Wanderlingh, U. *J. Appl. Polym. Sci.* **2015**, *132*, 7.
40. Norajit, K.; Kim, K. M.; Ryu, G. H. *J. Food Eng.* **2010**, *98*, 377.
41. Wang, Q.; Wang, Q.; Wang, X.; Padua, G. W. *J. Agric. Food. Chem.* **2006**, *54*, 517.
42. Vogler, E. A. *Adv. Colloid Interface Sci.* **1998**, *74*, 69.
43. Alcântara, A. C. S.; Aranda, P.; Darder, M.; Ruiz-Hitzky, E. *J. Mater. Chem.* **2010**, *20*, 9495.
44. Park, Y.-I.; Lee, K.-H. *J. Appl. Polym. Sci.* **2001**, *80*, 1785.
45. Nakabayashi, M.; Okabe, K.; Fujisawa, E.; Hirayama, Y.; Kazama, S.; Matsumiya, N.; Takagi, K.; Mano, H.; Haraya, K.; Kamizawa, C. *Energy Convers. Manage.* **1995**, *36*, 419.
46. Zou, J.; Ho, W. S. W. *J. Membr. Sci.* **2006**, *286*, 310.
47. Lannung, A. *J. Am. Chem. Soc.* **1930**, *52*, 68.
48. Weast, R. C. CRC Handbook of Chemistry and Physics, 52th ed.; CRC Press: Cleveland, **1971**.
49. Wu, J.; Yuan, Q. *J. Membr. Sci.* **2002**, *204*, 185.
50. Taylor, N. W.; Zobel, H. F.; Hellman, N. N.; Senti, F. R. *J. Phys. Chem.* **1959**, *63*, 599.